SUPPLEMENTARY INFORMATION

ADDITIONAL EXAMPLES

This Supplement contains figures that provide both context and additional examples of the glass samples. These are referenced in the main text and include context for the landscape and glass occurrences at the Puquio Nuñez (**Figures S-1**) and Chipana (**Figures S-2, S-3**) sites; further examples indicative of dynamic emplacement of the glasses (**Figures S-4, S-5, S-6**); trapped paleo-flora (**Figure S-7**); stratigraphy and association with paleo grasses (**Figures S-8, S-9**). Further details about the captured meteoritic fragments and assemblages in the glass is given below, including evidence (**Figure S-10**).

METEORITIC COMPONENTS

Methods

Polished, unpolished, carbon-coated, and non-contaminated samples in this study were analyzed using backscattered electron microscopy on a Hitachi SU-3500 VP-SEM at Fernbank Science Center employing accelerating voltages between 15 kV and 25 kV. Chemical compositions of selected phases were determined using an EDAX Element EDS detector, an accelerating voltage of 15kV, and a working distance of 10 mm. Selected samples were investigated using a field emission SEM (FEI Teneo) with a 150 mm Oxford XMax^N EDS detector. EDS compositions were based on comparisons to Smithsonian glass reference standards NMNH 111240-52, VG-2, USMN 2212, NMNH 72854, VG-568 with <1 wt% error on SiO_2.

Trapped in Pica Glass

Pica glass contains abundant silt-sized and finer meteoritic particles (fragments) that occur as individual phases and complex assemblages typically associated with vesicles. They range from Ni-bearing troilite (FeS, **Figure S-10A**) buchwaldite ($NaCaPO_4$, **Figure S-10B**), and oldhamite (CaS) to rock fragments composed of Mg-Fe silicates, corundum-bearing perovskite ($CaTiO_3$), and serpentinite. CAIs occur with melilite corona surrounding cores of carbonate and Ca-rich silicates (wollastonite and monticellite). Most abundant are Fe-sulfide assemblages composed of hexagonal platelets of Ni-rich and Ni-poor troilite and pyrrhotite often with Ni-rich Cu-Fe sulfide rims (**Figure S-10A**). EDS analyses of the rims on Ni-bearing troilite/pyrrhotite grains (**Figure S-10C**) indicate that they are composed of near stoichiometric cubanite ($CuFe_2S_3$).

Although cubanite and many other commonly meteoritic minerals have terrestrial counterparts, the details of their size, texture and associations often are distinctly different in the extraterrestrial cases. The occurrence of cubanite overgrowths on fine pyrrhotite/troilite grains is unmistakably similar to those observed for Wild 2 and Orgueil samples by Alfing et al. (2019), as well as the experimental analogs performed to replicate Stardust observations Berger, et al. (2015). While there could be as yet unobserved similar occurrences in terrestrial settings, this possibility would ignore the intimate association of these phases with phases such as buchwaldite (a uniquely meteoritic phase) and, where found, is associated with iron sulfides in meteorites. Note that Roperch et al. (2017) did not find any evidence of nickel in the examined troilite, which contributed to their conclusion that the glasses were not the result of a bolide. Moderately volatile meteoritic components such as nickel and copper, however, would be expected to fractionate during ultra-high temperature heating events, thereby accounting for the presence of some nickel-poor troilites.

Initially the exogenic component seemed to fall into three groups: 1) an iron-like component represented by Fe-Ni, Fe-Ni sulfides, buchwaldite, and schreibersite; 2) a primitive carbonaceous component represented by CAI-like particles and AOIs; and 3) a mafic silicate component represented by enstatite, diopside, Ca-rich plagioclase, and halogen-rich albite, all typically associated with iron sulfides and/or chlorapatite. This classification only serves to sort the variety of clasts that are identified in the glass but does not account for every phase. However, based on the expectation that an airburst would more easily result from a collision with a weak, volatile-rich fragmental body, this scheme was consistent with a working hypothesis that the bolide was similar to a body such as Bennu, which likely originated as a cometary body.

The abundant iron-sulfide/iron-nickel sulfide/iron-copper-nickel sulfide assemblages (fragments) that coat the walls of many vesicles provide key insights into the nature of the Pica bolide. Berger et al. (2011, 2015) performed controlled laboratory experiments (e.g., controlled pH, temperature, and oxygen fugacity) in order to understand the aqueous alteration on comets as represented by the Stardust samples returned from 81P/Wild and the CI primitive chondrite Orgueil. By simulating the hydrothermal conditions that likely existed on the CI-chondrite parent body (and comets), they were able to produce cubanite in nearly all the experiments. The Pica sulfides not only are very similar in chemistry and morphology to those reported in both CIs and cometary material, but the entire suite of exogenic minerals also compare quite well with CIs, or a combination of CIs and CVs. As a result, a cometary body is the most likely candidate to have been the Pica impactor.

If the sulfide assemblages were initially identical to CI sulfides, then some of these sulfides could have been altered during the airburst event over Chile. First, there is some evidence that nickel was mobilized from some grains at temperatures exceeding 2000ºC during melting. Second, most of the sulfide platelets exhibit pervasive planar fracturing, which we can imagine could be imparted by rapid mechanical or thermal shock. But some rare grains show clear evidence of metamorphism by a transient high-pressure shock wave (**Figure S-10B**). According to Bennett and McSween (1996), polycrystallinity develops most commonly starting at shock stage 4, corresponding to approximately 30 GPa. This grain has developed polycrystallinity, and the fracturing subsequently followed the crystallographic control of each oriented domain. Nevertheless, the presence of preserved cubanite in vesicles within the glass also requires late-stage entrapment of unshocked trailing minerals because cubanite changes irreversibly to another crystalline form at 210°C.

Strong winds and vortices would entrain and loft melts that mix with trailing meteoritic clasts before quenching and returning to the surface nearby. For example, a recent study (Silber et al., 2018) modeled the atmospheric response to a 16 Mt air blast from an object entering at 45° and bursting at an altitude of 12 km. The resulting winds exceeded 100 m/s over an area of 25 km^2. Consequently, the trapped meteoritic minerals record a wide range of conditions. The ubiquitous occurrence of unmelted meteoritic assemblages within vesicles also requires that particles were entrained immediately after initial melting, consistent with meteoritic debris in the trailing wake.

POSSIBLE DISTAL MATERIALS

The Pica glasses may be related to magnetic spherules, titanomagnetite grains, and enhanced iridium found concentrated within similar-age black organic mats farther south (Pigati et al., 2012). At Quebrada del Chaco (about 250 km south of the Pica glasses), the titanomagnetite grains have a concentration of 36.8 g kg^{-1} in a 12.3 ka black mat that greatly exceeds the concentration (2.1 g/kg^{-1}) in an older, 13.0 ka mat at El Sato about 150 km farther to the south. Magnetic spherules exhibit an even higher concentration of 993 g kg^{-1} at the base of another black mat at Quebrada del Chaco but date to 11.5 ka. Iridium levels spike within the mats but occur at different times (11.5 ka to 15.9 ka). Pigati et al. (2012) concluded that the iridium spikes and micro-particles could not be related the proposed Younger Dryas Boundary bolide event (12.8 ka), but they could represent distal Pica components affected by downward mobility during soil formation and changing environmental conditions (e.g., Martin-Peinado and Rodriguez-Tovar, 2010).

Much farther away at Osorno in Patagonia Chile (2600 km to the south), small (tens of microns) melt-glass spherules have been found in sediments correlated with the YDB boundary (Pino et al., 2019). Independent analyses of a few dozen magnetic particles with meteoritic signatures (high-temperature condensates, relict zircons, and attached sediments) from this layer revealed compositions and fragments of iron sulfides with copper-rich rim very similar to the Pica glasses (Harris and Schultz, 2019). It remains unclear, however, if these Osorno particles correlate with the proposed YD Boundary event (12.8 ka) or are actually related to the younger Pica glasses, as suggested by their common characteristics. Just as at Quebrada el Chaco, the Osorno particles could have mobilized to a lower stratigraphic level and are actually related to the younger (<12.3 – 11.5 ka) Pica glasses.

The dispersal of small melt particles far from the epicenter of a near-surface airburst would require lofting by upward-directed plumes or rising vortices (e.g., Boslough and Crawford, 2008) that could be carried by high-level winds.

PROPOSED ORIGIN BY GRASS FIRES

A prior study (Roperch et al., 2017) concluded that the Pica glasses resulted from intense grass fires based on the following observations: (a) reported absence of high-temperature products;

(b) absence of meteoritic signatures; (c) inferred differences in the age of glass formation at different sites based on the ^{14}C ages of soils and paleomagnetic data; and (d) association with paleo-grasses (**Fig. S7;** also see Roperch et al., 2017). As described above, however, these glasses not only exhibit evidence (e.g., baddeleyite) for extreme temperatures (a) but also contain abundant mineral grains and rock fragments of the same extraterrestrial source including Ni-troilite (b) in widely separated samples. The range in ages (c) is attributed to different ages of surface soils on which the glasses occur, and not the age of the glass-forming event. Moreover, the observed differences in the remanent magnetic inclinations and paleointensities, up to 100° and 28 μT, can be explained by the effects of ionized gas associated with an impact or a low-altitude fireball that partly shielded the melted soils from the earth's magnetic field as they passed through the Curie point (Crawford and Schultz, 1991; Boslough and Crawford, 2008).

Finally, an origin by fires fusing dried grasses and/or phytolith-rich soils (inference d) is inconsistent with four key observations. First, when found in situ, a silty clay layer separates the glass from the paleo-grass layer (**Figures S-8, S-9**). Second, glasses occur on top of different lithologies, in places without any association with phytolith-rich soils. Third, the volume of glass could not be accommodated by the fusion of phytolith-rich soils and silicified grass, as it would require grass quantities that greatly exceed that available in these desert wetlands, and cannot explain those occurrences where those materials are absent. Fourth, the compositional variation in the glass is consistent with that of the underlying or nearby soils, rather than a single source such as grass or phytolith-rich soil.

Bennett M. E. I. and McSween H. Y. J., 1996, Shock features in iron-nickel and troilite of L-group ordinary chondrites: Meteoritics and Planetary Science, v. 31, p. 255–264.

Crawford, D.A. and Schultz, P.H., 1991, Laboratory investigations of impact-generated plasma:

Journal Geophysical Research, v. 96, no. E3, p. 18,807–18, 817.

Harris, R. S. and Schultz, P. H., 2019, Are Ti-rich particles in Late Pleistocene sediments from Patagonia ejecta from an Atacama airburst?: Lunar and Planetary Science L, abstract 2132.

Martin-Peinado, F. J and Rodriguez-Tovar, F. J., 2010, Mobility of iridium in terrestrial environments: Implications for the interpretation of impact-related mass-extinctions: Geochimica et Cosmochimica Acta, v. 74, Issue 15, p. 4531-4542

Pigati et al., J. S., Latorre, C., Rech, J. A., Betancourt, J. L., Martinez, K. E., and Butahn, J. R., 2012, Accumulation of impact markers in desert wetlands and implications for the Younger Dryas impact hypothesis: Proceedings of the National Academy of Sciences, v. 109, 7208-7212. ww.pnas.org/cgi/doi/10.1073/pnas.1200296109.

Pino, M., Abarzúa, A. M., Astorga, G., Martel-Cea, A., Cossio-Monecinoa, N., Navarro, R. E., Lira, Maria P. L., Labarca, R., LeCompte, M. A., Adedeji, V., Moore, C. R., Bunch, T. E., Mooney, C., Wolbach, W. S., West, A., and Kennett, J. P., 2009, Sedimentary record from Patagonia, southern Chile supports cosmic triggering of biomass burning, climate change, and megafaunal extinctions at 12.8 ka: Scientific Reports, v.9, no. 1, p. 1–27.

Figure S-1A: Numerous glass slabs are scattered across the top of mounds and small plateaus (arrows) as illustrated in this areal view of the Puquio de Nuñez (PN) area south of Pica (20° 35' S and 69° 21.6'W). Mobile dunes between the mounds/plateaus partly cover fossilized paleo-flora and in some cases isolated clusters of glasses. Bits and pieces of broken fossilized paleo-flora and cobbles typically occur near or just below the surface. **Figure S-1B:** The foreground area typifies the clusters of glass slabs scattered across the top of a small mound at the PN site, along with other concentrations in the distance (arrows). Some clusters and isolated glasses also occur in the lower lying areas emerging between active sand dunes.

Figure S-2A: Glass strewn fields 30 km to the south of Puquio de Nuñez occur on overbank deposits of Quebrada Chipana (QC) near 20° 54' S and 69° 19.5'W. This areal view reveals small channels cutting between clusters of the deposits composed of glass fragments mixed with clay. White arrows identify people for scale. **Figure S-2B:** QC glasses are scattered across a thin layer of clay that cover paleo-grasses (reddish area lower right). Glassy masses range from a few cm to well over 10 cm across (footprint at center bottom and GSA tape-measure provide a scale for the foreground). Most of the large glasses cooled as single masses, whereas some of the smaller masses represent scattered fragments. Other concentrations occur in the distance on top of the low-relief mounds.

Figure S-3A: This stereo view reveals a linear cluster of glasses mixed with clays at QC. They are emplaced on top of Pleistocene alluvial deposits characterized by innumerable, small faceted clasts. The cluster of glass at lower right is about 10 cm across. It remains unclear if the mounds represent ballistically transported glass and clays or relict deposits remaining after later aeolian and fluvial processes. **Figure S-3B:** Clusters of glass (yellow arrows) and clay were deposited on contrasting alluvium reflecting different transport rates, e.g., larger rounded pebbles (lower left) or small faceted clasts (surrounding deposits). Some pebbles are fractured (white arrows) due to thermal fracturing or perhaps related to emplacement.

Figure S-4A: Many large glasses appear to have been transported in a flow or emplaced ballistically as illustrated in this example at Chipana. The view here provides a broader view of the glass sample shown in Figure 2A (main text) and reveals that the central mass is surrounded by fragments that shed (spalled?) during emplacement along with a trail of debris extending more than 2 m (right). **Figure S-4B:** This large (0.3 m) glass at Chipana partly rolled during emplacement (side shown was originally on the bottom). After the mass had partly quenched to form a smooth surface, the embedded soils fused to the bottom and tongue-like lobes indicate that the glass slab slid along the surface and continued forward and upward before resting.

Figure S-4C: A closer view of the glass in Figure S-4B reveals embedded soils and paleo-grass imprints fused before completely quenched.

Figure S-5: A long, twisted glass sample (from QC) exhibits a smooth, quenched side (**A**) and a pitted, vesicular side (**B**) of dynamic emplacement. The larger mass at left (**A**) has numerous paleograss imprints indicating that the mass had not yet fully quenched inside.

Figure S-6A: This complex arrow-shaped glass slab (PN region) illustrates the collection of smaller melt glass globs into a larger mass, as well as the effects of dynamic transport and emplacement. Overlapping glass packets (stringers) likely indicate break-outs of a partly cooled melt injected into a wet surface. Coin is 2 cm in diameter. **Figure S-6B:** A portion of the same glass slab shown in Figure S-5A (lower right) with different lighting clearly reveals individual twisted and folded stringers. The stringers are interpreted as melted packets of soil that had fused together and partly quenched before hitting the surface; as a result, the entire mass folded over. The vitreous surface and absence of soils embedded in the glass (soils shown are loosely attached or embedded) require that this piece rapidly quenched before emplacement.

Figure S-7: Some glasses at Chapana have casts of silicified twigs, some of which remain (**A**). This relationship indicates that the glass must have been transported after melt formation and incorporated the twigs prior to complete quenching. At Puquio de Nuñez (**B**), many glasses have two sides: one (upper surface) with a smooth quench surface (not shown); the other (underside) with flow lines and paleo-grass imprints indicating motion during formation (**C** detail of **B**).

Figure S-8: A section under the surface deposits of glass reveals a clay layer separating the glasses from the layer of paleo-grasses at Chipana. This provides evidence that the surface glasses could not have been made from intense fires from the grasses below. In addition, the paleo-environment in this area could not have provided enough dried grass for a fuel for fires sufficient to produce the observed large glass masses.

Figure S-9: A context (**A**) and close (**B**) view of a cross-section below the surface glasses (white arrows) at the Chipana site reveals the silicified paleo-grasses (yellow arrows) separated by a clay layer. The context view shows the continuous layer of matted paleo-grasses. The closer view (**B**) reveals freshly exposed lithified grass as well as the clay with some darkened clumps and glasses above.

Figure S-10A. Electron backscattered (BSE) photomicrograph of Fe-Ni-Cu sulfide grains on the wall of a vesicle in Pica glass. The assemblage is very similar to sulfide assemblages documented in CI meteorites (Alfing et al., 2019), and the Cu-rich overgrowths are the same as those discussed by Berger et al. (2011, 2015) that occur from aqueous alteration on comets.

Figure S-10B. Electron backscattered (BSE) photomicrograph of acicular buchwaldite that typically occurs with Fe±Ni sulfides in Pica glasses. Buchwaldite is a uniquely meteoritic phase and where found in meteorites is associated with iron sulfides, as it is here. **Figure S-10C.** Electron backscattered (BSE) photomicrograph of troilite grain in Pica glass. The grain has developed polycrystallinity likely due to shock metamorphism. The planar fractures follow the crystallography of each subgrain.

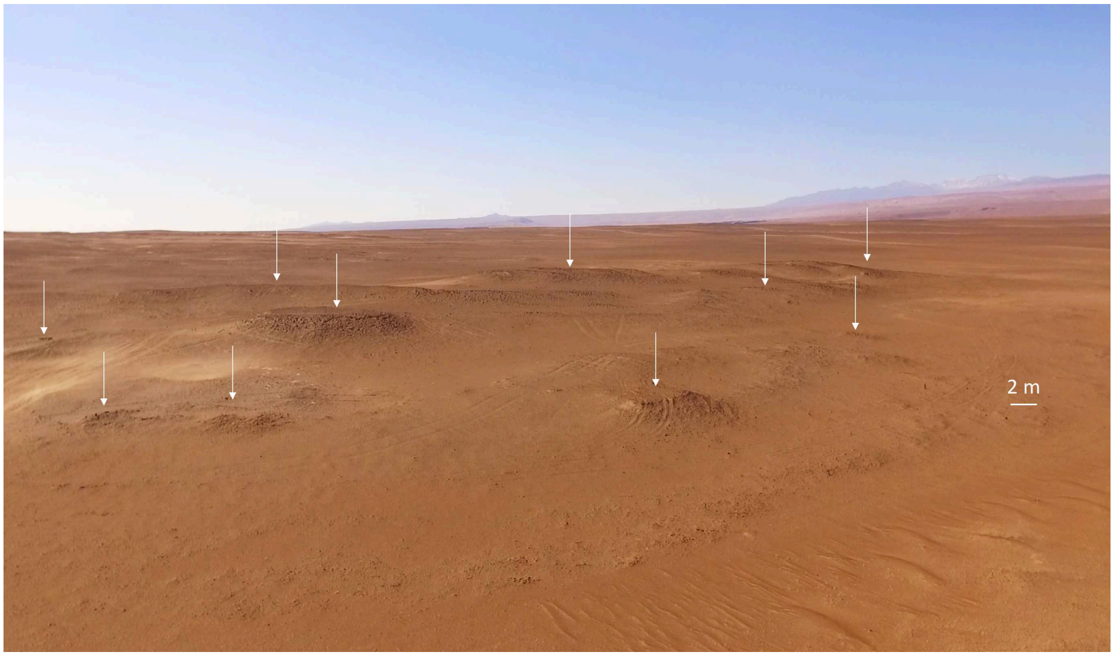

A

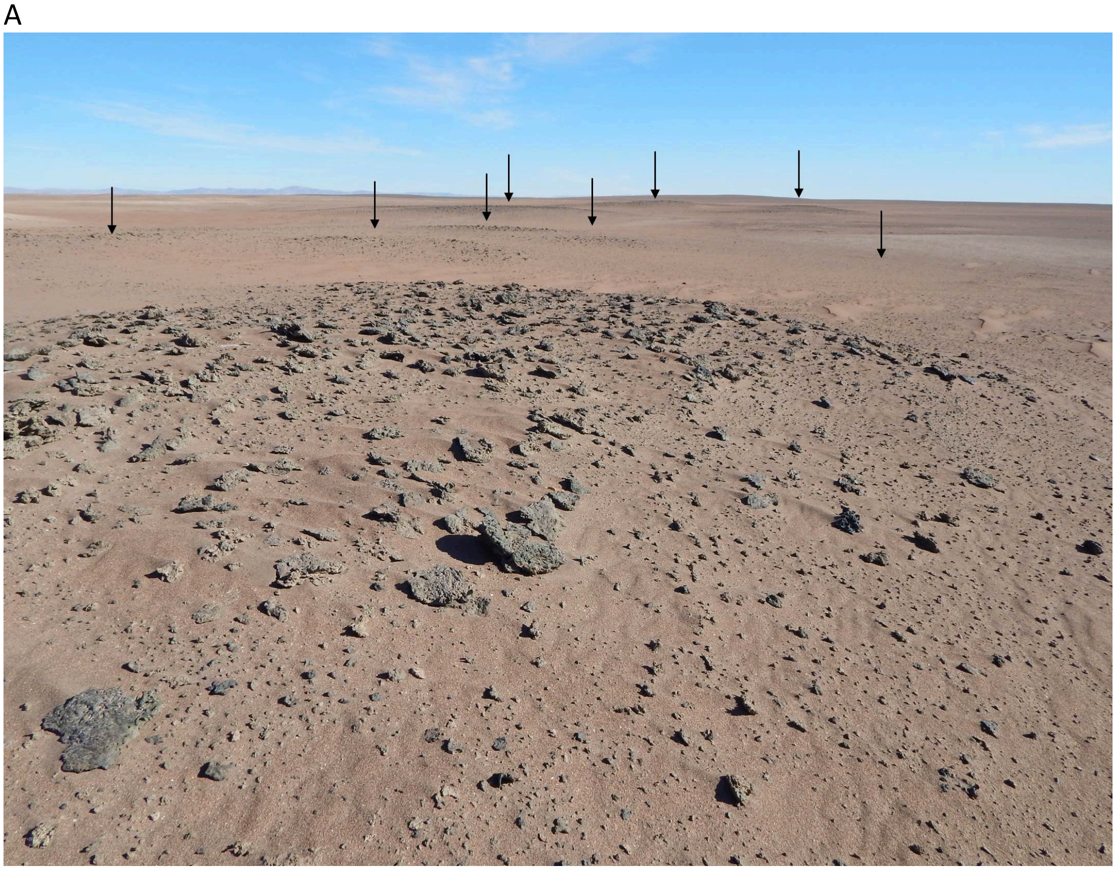
B

Fig. S-1


A
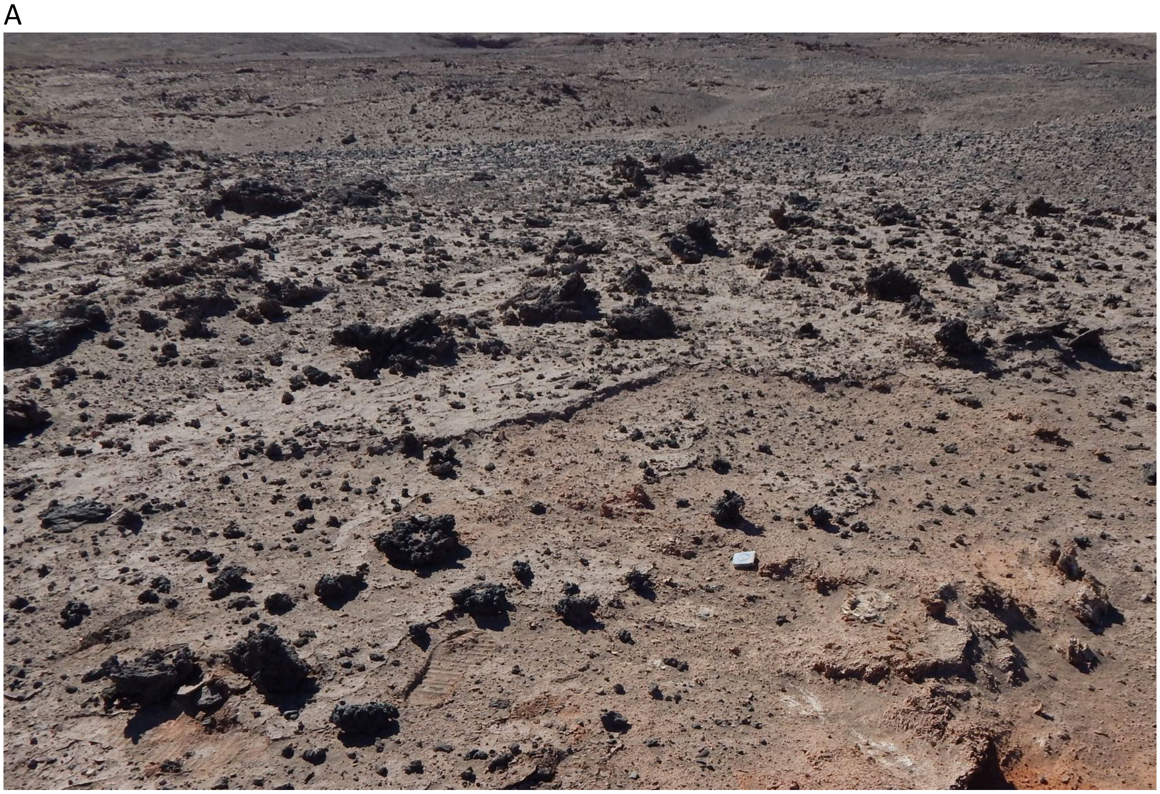
B
Fig. S-2

A

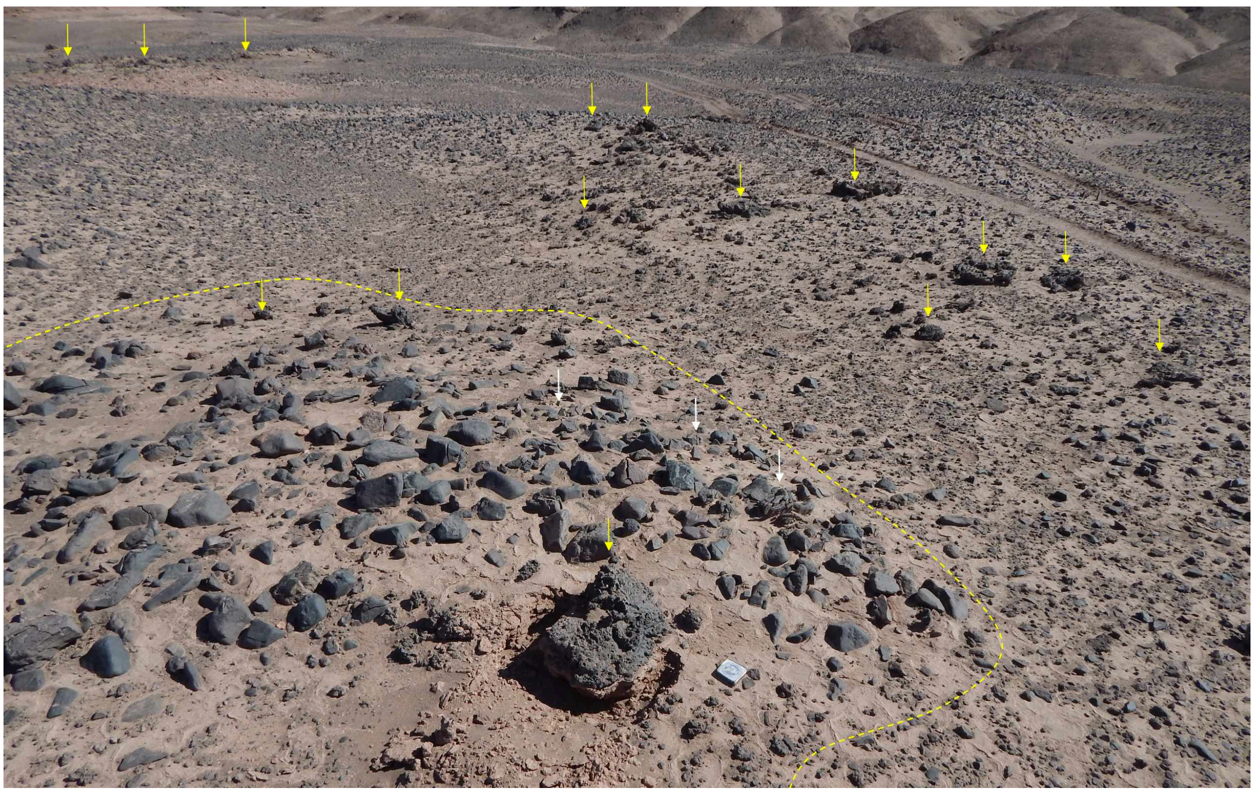

B

Fig. S-3

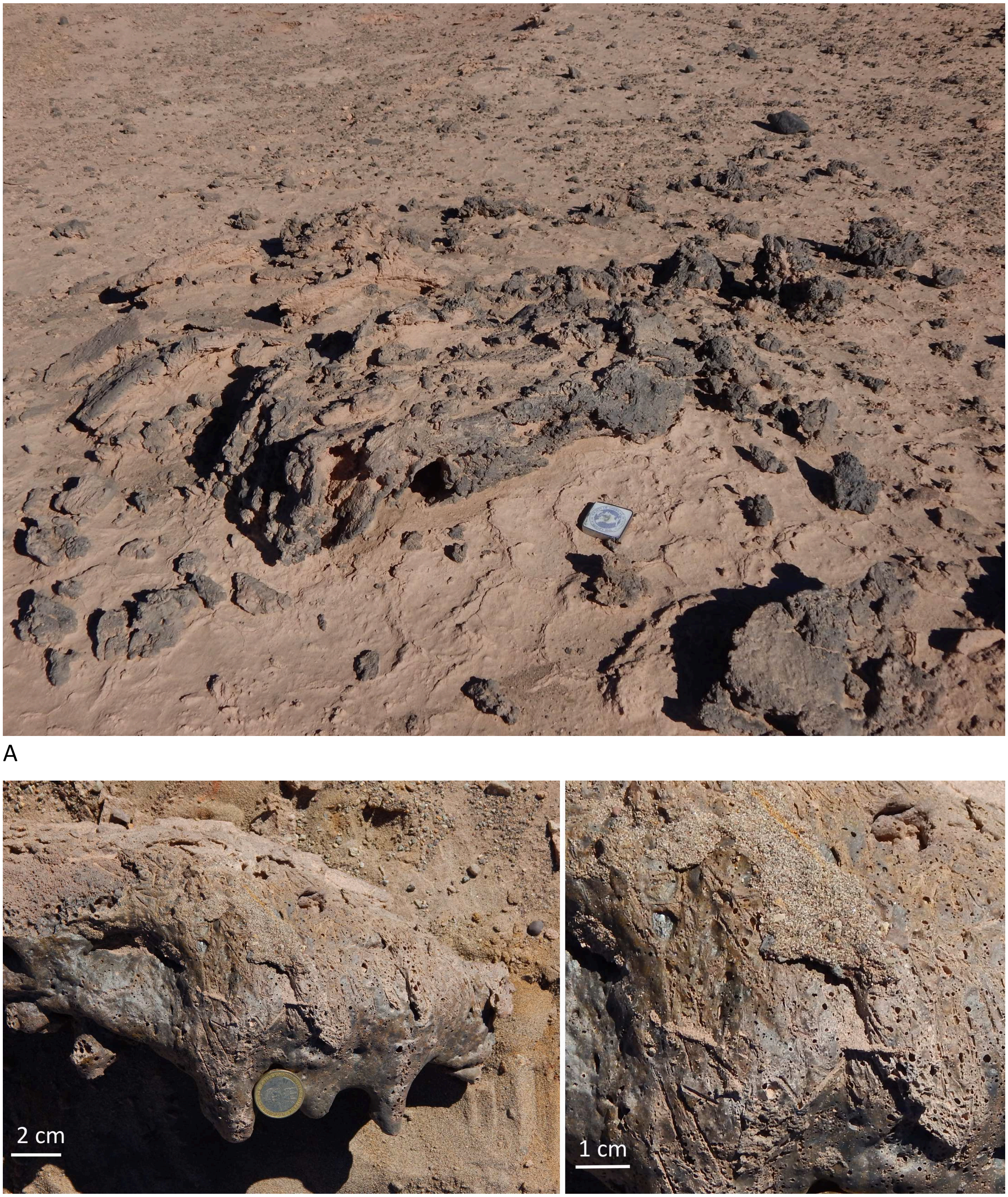

A

B

C

Fig. S-4

A

B

Fig. S-5

A

B

Fig. S-6

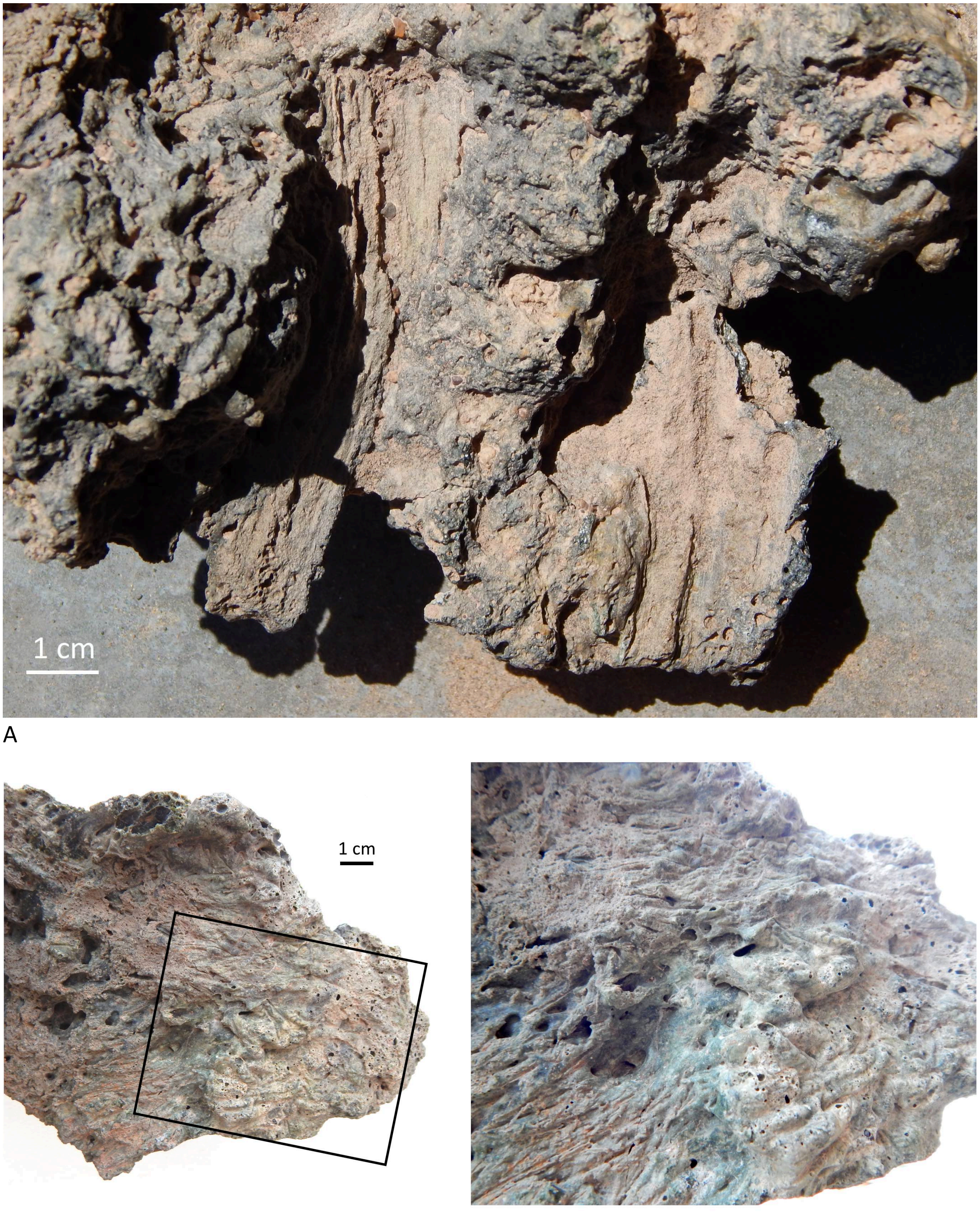

Fig. S-7

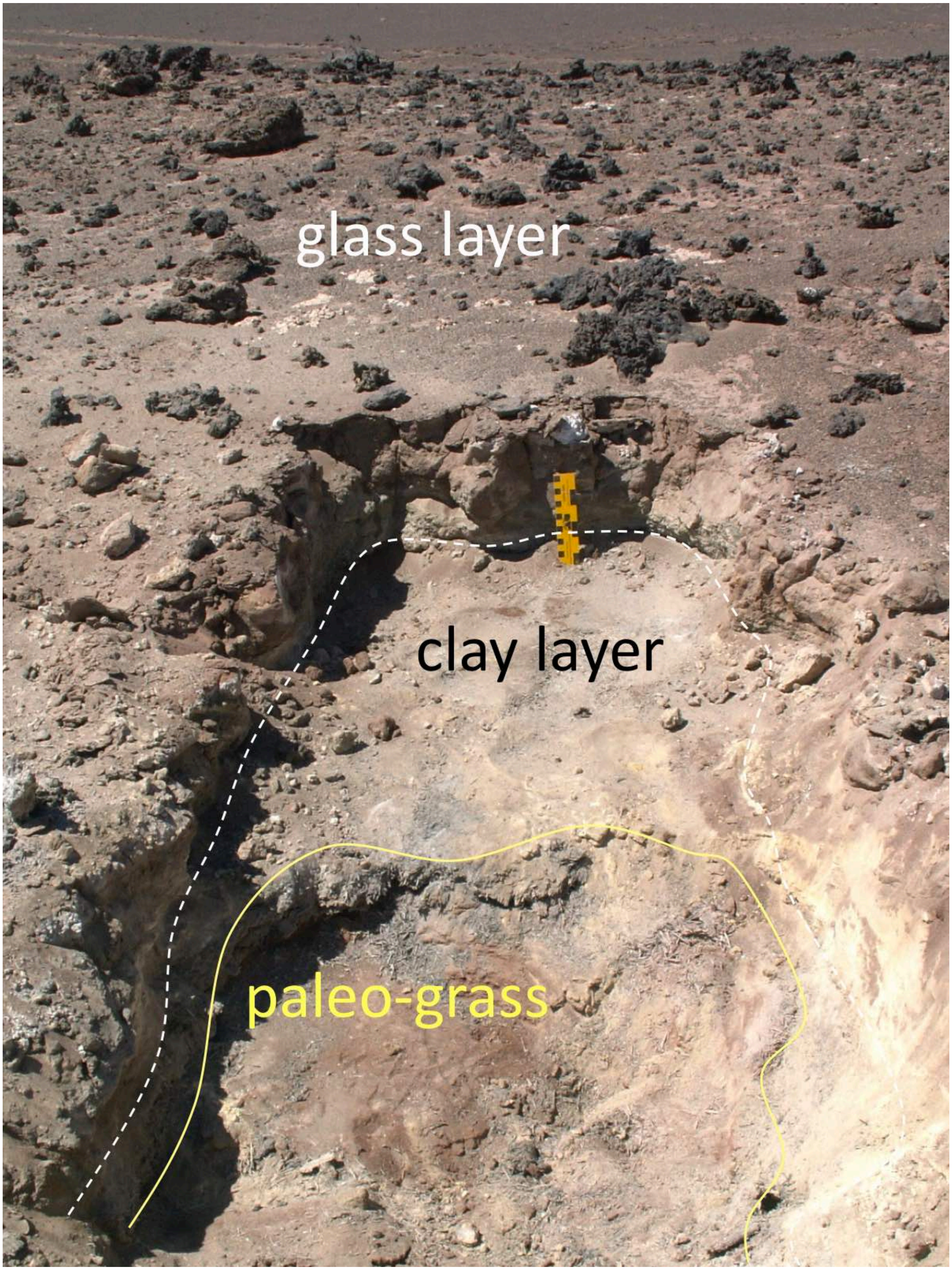

Fig. S-8

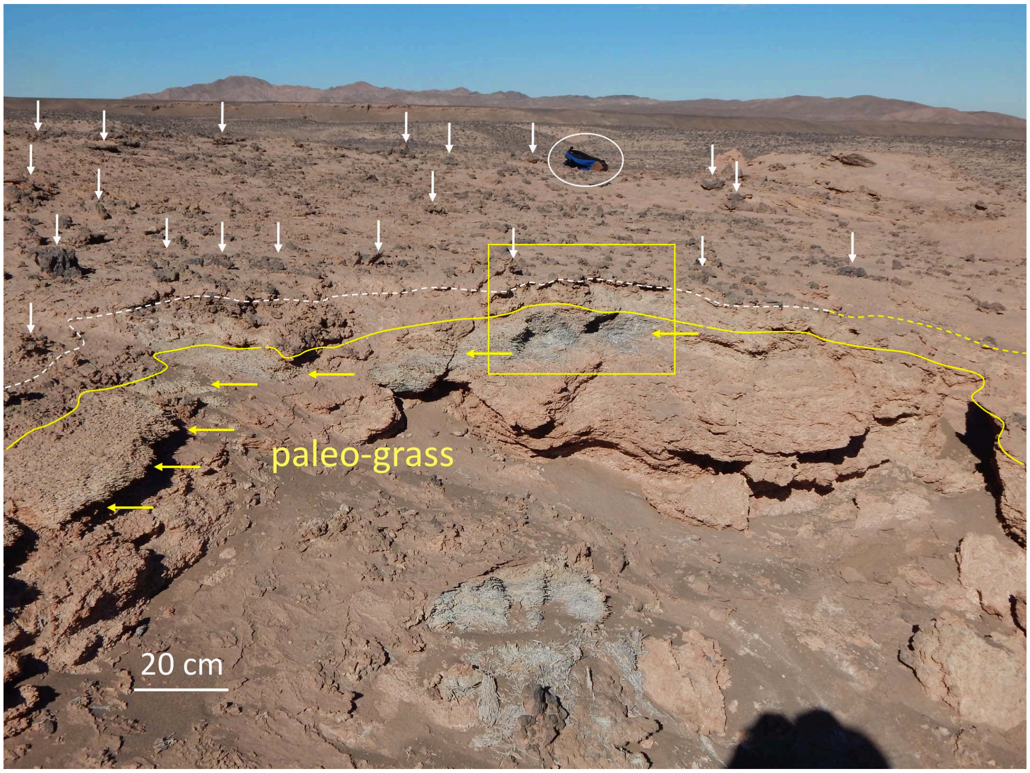

A

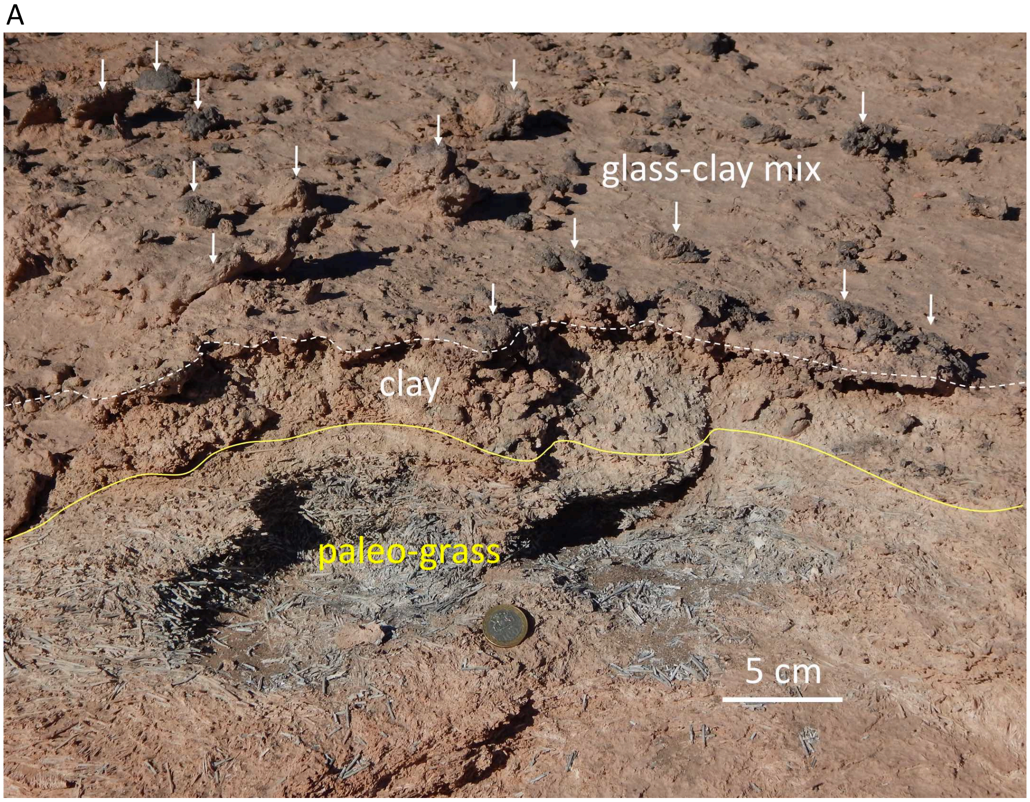

B

Fig. S-9

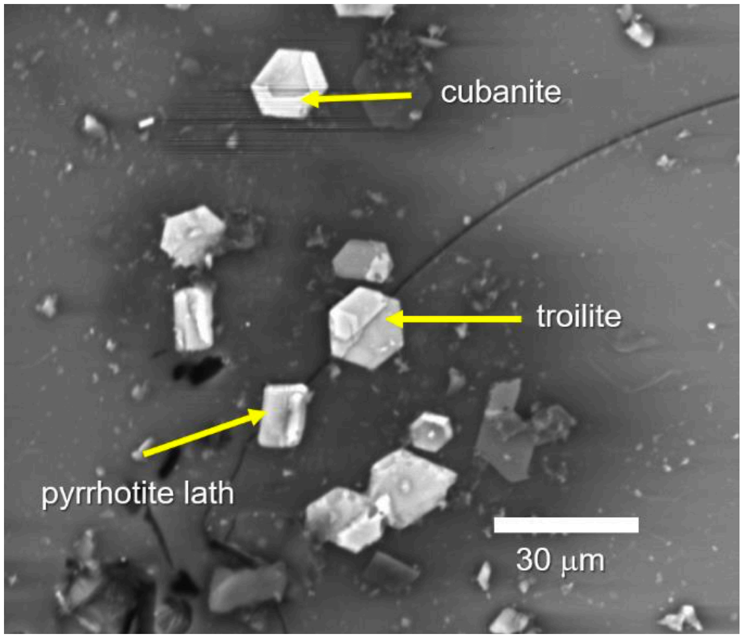
cubanite
troilite
pyrrhotite lath
30 μm

A

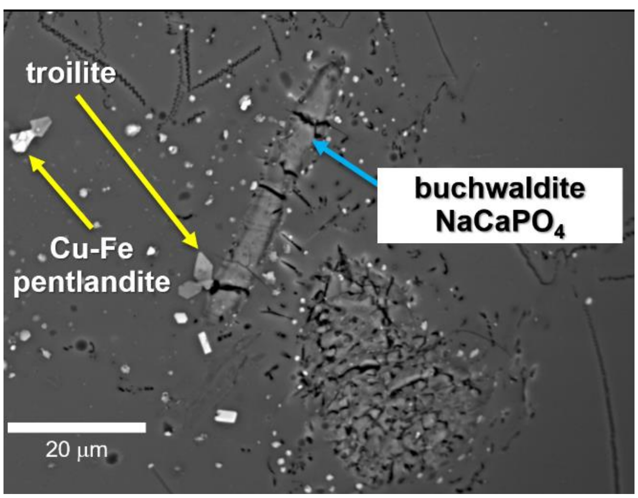
troilite
buchwaldite
NaCaPO4
Cu-Fe
pentlandite
20 μm

B

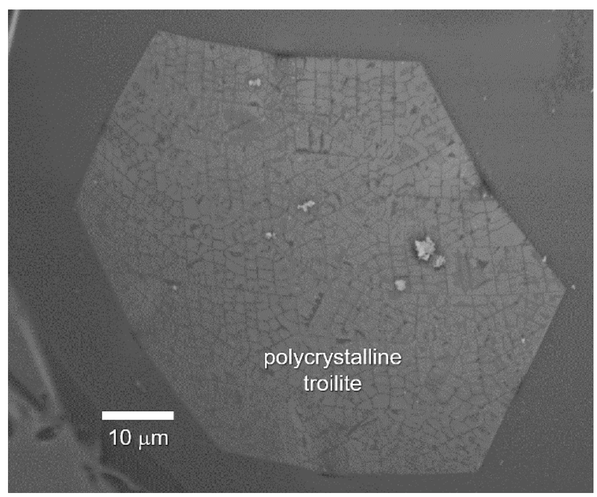
polycrystalline
troilite
10 μm

C